

# Is Image Size Important? A Robustness Comparison of Deep Learning Methods for Multi-scale Cell Image Classification Tasks: from Convolutional Neural Networks to Visual Transformers

Wanli Liu<sup>a</sup>, Chen Li<sup>a,\*</sup>, Hongzan Sun<sup>b</sup>, Weiming Hu<sup>a</sup>, Haoyuan Chen<sup>a</sup>, Changhao Sun<sup>a</sup>, Marcin Grzegorzek<sup>c</sup>

<sup>a</sup>*Microscopic Image and Medical Image Analysis Group, MBIE College, Northeastern University, 110169, Shenyang, PR China*

<sup>b</sup>*China Medical University, 110001, Shenyang, PR China*

<sup>c</sup>*University of Lübeck, Germany*

---

## Abstract

Cervical cancer is a very common and fatal cancer in women, but it can be prevented through early examination and treatment. Cytopathology images are often used to screen for cancer. Then, because of the possibility of artificial errors due to the large number of this method, the computer-aided diagnosis system based on deep learning is developed. The image input required by the deep learning method is usually consistent, but the size of the clinical medical image is inconsistent. The internal information is lost after resizing the image directly, so it is unreasonable. A lot of research is to directly resize the image, and the results are still robust. In order to find a reasonable explanation, 22 deep learning models are used to process images of different scales, and experiments are conducted on the SIPaKMeD dataset. The conclusion is that the deep learning method is very robust to the size changes of images. This conclusion is also validated on the Herlev dataset.

**Keywords:** Cervical cancer, Deep learning, Pap smear, Multi-scale image, Visual Transformer, Robustness comparison

---

## 1. Introduction

Cancer is the deadliest disease in the growth process of the human body. Approximately 9.6 million people die from cancer every year [1]. According to the latest world cancer statistics, cervical cancer is the seventh most common cancer in the world, and it ranks fourth in the incidence of women. In developing and low-income countries, hundreds of thousands of women lose their lives every year because of cervical cancer [2]. These situations occur because these women lack hygiene knowledge and the medical security conditions in these countries are not very good. According to research findings, the culprit of cervical cancer is human papillomavirus (HPV) [3].

HPV is the most common sexually transmitted virus in the world. Regardless of gender, if people

have very active sexual behaviors, they are likely to be infected with hpv virus [4, 1]. According to the research surface, about 200 types of HPV viruses are discovered so far. There are 13 high-risk types among these types of HPV viruses, and 70% of cervical cancers are HPV type 16 and 18 [5, 6]. 24% of women are detected to be infected with HPV type 16, and 9% of women are detected to be infected with HPV type 18 [5, 7, 8]. Most of the causes of cervical cancer are premature first sexual intercourse, intercourse with multiple partners, pregnancy, weak immunity, smoking, oral contraceptives, and unhygienic menstruation. Common symptoms of cervical cancer are abnormal vaginal bleeding, vaginal discharge, and moderate pain during sexual intercourse [9]. If cervical cancer is detected in time and given appropriate treatment, cervical cancer can be cured [10].

Cervical cytopathology is usually used to diagnose cervical malignancies. Because the cost of cer-

---

\*Corresponding author

Email address: lichen201096@hotmail.com (Chen Li)

vical cytopathological examination is relatively low, it is convenient for general investigation [10, 11]. The traditional detection process is to collect cells from the patient’s cervical squamous column with a brush or spatula, and then smear cells on a glass slide. A professional doctor observes it under a microscope and determine whether there is any disease. However, a large number of manual screening is very troublesome and time-consuming. And it is prone to artificial error, because there are thousands of cells in different directions and superimposed on each slide [12]. This problem needs a solution urgently.

An automatic computer-aided diagnosis system (CAD) that can analyse pap slices rapidly and accurately is developed. In addition, the computerized system can also process a large number of images, which provides convenience for clinical follow-up, comparative research and personalized medicine [13]. People conduct in-depth research on the CAD system. This system can automatically detect and classify abnormal cells in cytopathological images [14]. Nowadays, deep learning technology is widely used in computer vision, medical image, natural language processing and other fields [15, 16]. In traditional CAD systems, the main limitation is that the features are manually extracted, which cannot make the classification results effectively. However, deep learning technology is an end-to-end method that makes it possible to automatically learn features [17]. The performance of deep learning technology in image analysis is better than traditional methods and machine learning. But training a deep learning model requires a considerable number of labeled data sets [18]. There is a key question about deep learning is that although it provides better results, its characteristics are incomprehensible to humans [19].

The deep learning programs currently used in the field of medical image analysis are all proven and most efficient algorithms. Convolutional Neural Network (CNN) is a very popular deep architecture. It is widely used in image segmentation and classification [15]. In the cell classification task, a CNN model classifies normal cells and abnormal cells by extracting hierarchical features from the original image [20]. Recently, Visual Transformer (VT) that applies the Transformer architecture for processing NLP tasks to the field of computer vision suddenly appears. There is a VT model called ViT, which has better results than the latest convolutional network under the premise of pre-training

with a large amount of data, and the computing resources required for training are greatly reduced. But when the amount of data is small, the effect may not be ideal [21].

The input of the deep learning models is consistent, but the size of clinical cervical cell images is mostly inconsistent. The internal information is lost after resizing the image directly, so it is unreasonable. But most studies directly resize the cell images, and their results are still robust. So this paper is proposed to find a reasonable explanation for this situation, where a robustness comparison of deep learning methods for multi-scale cell image classification tasks is carried out to find the answer of “is image size important or not for deep learning classification?”

In this paper, an experimental platform for the robustness comparison of deep learning methods in multi-scale cell image classification tasks is built. The workflow of this method is shown as in Fig. 1. First, raw data from SIPaKMeD public dataset are used in this paper, including 4049 cervical cell images [22]. Then the raw data are standardized and centralized into standard data. After rotating 180 degrees, flipping left and right and flipping up and down, both the raw data and standard data are augmented to four times. The data without augmentation and data after augmentation are input into the deep learning models for training. Finally, the closed test images are input into the models for classification. The performance is evaluated by calculating the accuracy, precision, recall and F1-Score during the validation and testing phases.

In addition, in order to conduct a comparison experiment on the robustness of deep learning methods in multi-scale cell image classification tasks, 22 well-known deep learning models are selected for this experiment. 18 of the models are CNNs, including VGG11 [23], VGG13 [23], VGG16 [23], VGG19 [23], ResNet18 [24], ResNet34 [24], ResNet50 [24], ResNet101 [24], DenseNet121 [25], DenseNet169 [25], InceptionV3 [26], Xception [27], AlexNet [28], GoogLeNet [29], MobileNetV2 [30], ShuffleNetV2x1.0 [31], ShuffleNetV2x0.5 [31], InceptionResNetV1 [32]. The remaining four models are VTs, including ViT [21], BoTNet [33], DeiT [34], T2T-ViT [35].

The structure of this paper is as follows: Sec. 2 elaborates the related work of deep learning in the classification of cervical cells and deep learning technologies used in this paper. Sec. 3 describes the content of the open source database used in this

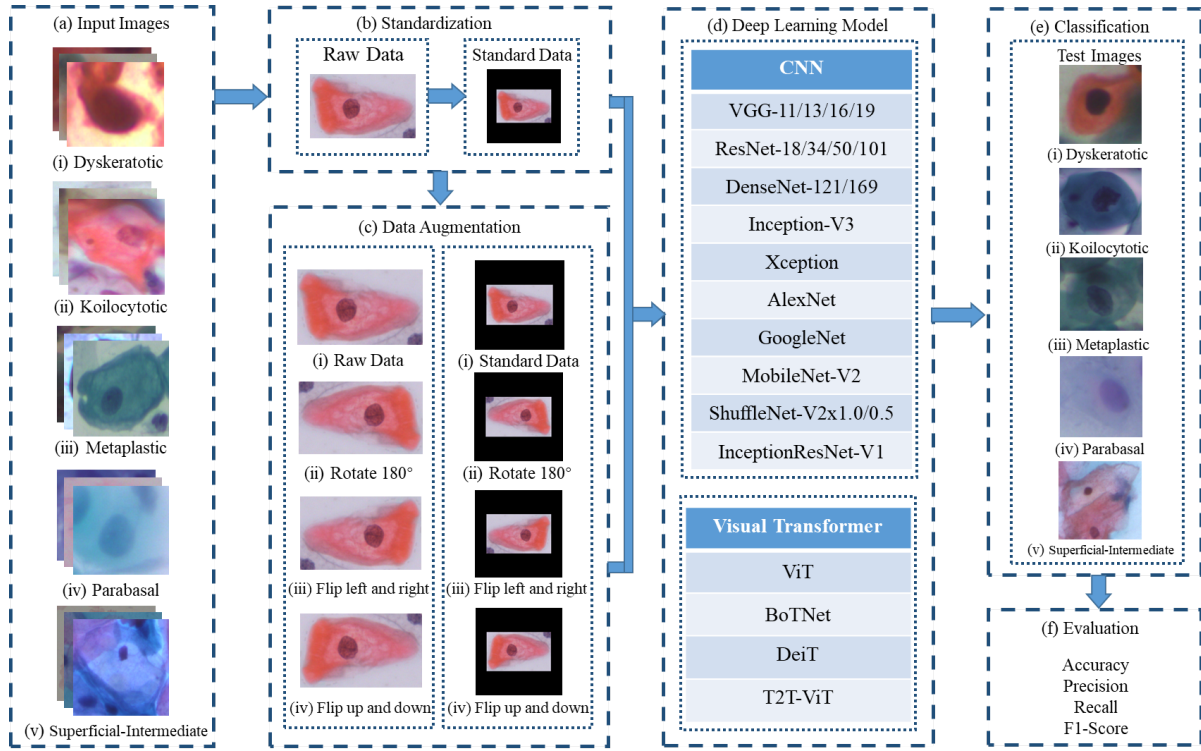


Figure 1: Workflow of a robustness comparison of deep learning methods for multiscale cell image classification.

method, the distribution of training, validation and test data, the method of data preprocessing, and deep learning models used. Sec. 4 explains the results of the comparative experiment and the analysis of the experimental results, including the experimental settings and evaluation indicators. Sec. 5 discusses based on the experimental results and the characteristics of models. Sec. 6 summarizes this paper and proposes the future work direction.

## 2. Related work

In this section, the related work of deep learning in cervical cell image classification tasks and the deep learning technologies used in this paper are briefly introduced. For detailed information, please refer to our previous review paper [13].

### 2.1. Applications of deep learning in cervical cell image classification

In [36], a private dataset containing 71344 cervical cell images is used. This paper proposes a model that combines CNN and machine learning to classify cervical cell images. Among them, VGG network is used to extract features, and the support

vector machine is used for classification. F1-Score of the classification result is 78%.

In [37], the paper uses the Herlev dataset, in which 70% of the images are used for training and 30% of the images are used for testing. This work uses the pre-trained AlexNet network for feature extraction, then transfers the features to SVM for two classification. The accuracy of this method reaches 99.19%.

In [38], VGG16 and ResNet architecture network are used to classify the CerviSCAN and Herlev dataset. CerviSCAN is a private database containing 12043 cervical cell images. In this paper, the input size of the image is adjusted to  $100 \times 100$  pixels. The F1-Score on VGGNet is 82%. And the F1-Score on ResNet is 83%.

A cervical cell analysis system for detection, segmentation, and classification is proposed in [39]. This work uses AlexNet for transfer learning to classify the Herlev dataset. They prove that segmentation is not necessarily related to classification. The accuracy of 2-class classification task and 7-class classification task reaches 99.3% and 93.75%

A comparative experiment using deep learning to classify cervical cell images is proposed

in [40]. This paper compares the performance of ResNet101, DenseNet161, AlexNet, VGG19\_bn, and SqueezeNet1\_1 on the Herlev dataset. Among them, DenseNet161 performs the best, with accuracy rates of 94.38% and 68.54% on 2-class classification and 7-class classification respectively.

In [41], InceptionV3, ResNet152 and Inception-ResNetV2 are used for feature concatenation and ensemble learning to classify cervical cells. This paper uses the 2D Hela dataset, Pap smear dataset and Hep-2 cell image dataset for performance evaluation. The comprehensive result of multiple models in this method is better than the result of a single model, and the accuracy rate on the Herlev dataset reaches 93.04%.

In [42], this paper transfers the pre-segmented cervical cell images into a compact version of VGG for classification. This compact version has only 7 layers, which reduces the computational cost. In this paper, the Herlev dataset is used for performance evaluation. The accuracy of 2-class classification is 98.1%. The accuracy of 7-class classification is 95.9%.

In [43], deep learning and transfer learning are applied to the binary classification task of cervical cell images for the first time. This paper uses the Herlev and HEMLBC dataset to evaluate performance. The HEMLBC dataset is a private database containing 2370 cervical cell images. The accuracy on the HEMLBC dataset is 98.6%. And the accuracy on the Herlev data set is 98.3%.

## 2.2. Deep learning technologies

VGG network is a CNN model proposed by Simonyan and Zisserman of Oxford University. The main innovation of this model is the use of deeper networks and smaller filters. The number of layers of the network can be 11, 13, 16, or 19. This work uses a  $3 \times 3$  filter, which has the same acceptance field as the  $7 \times 7$  filter, but the amount of parameters is greatly reduced [23].

AlexNet is proposed by Russakovsky et al, which introduces the ReLu activation function and successfully solves the saturation of Sigmoid. This method prevents overfitting by data augmentation and adding dropout layers, and makes the pooling layer overlap to enrich the features. The method also proposes the LRN layer to improve the generalization ability of the model [28].

ResNet network is proposed by He et al. In order to solve the problem of rapid decline in accuracy

as the number of network layers increases, it introduces residual block, as shown in Fig. 2. The input of the convolutional layer is  $X$ , and the residual mapping is  $F(x)$ , then the output  $Y = F(x) + X$ . The residual network can turn the deep network into a shallow network by setting other layers in the deep network as identity mapping. This solves the problem of network degradation [24].

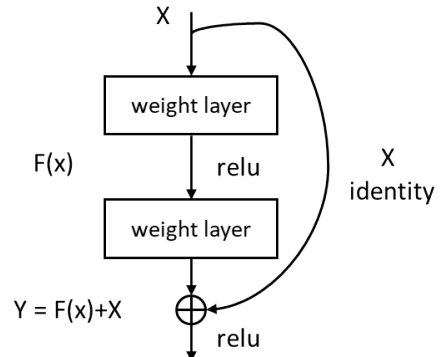


Figure 2: Residual block

A new convolutional network structure called DenseNet is proposed by Huang et al. It introduces a direct connection between any two layers with the same feature map size. DenseNet can scale to hundreds of layers and still be optimized. In the experiment, the accuracy of DenseNet continues to improve with more and more parameters. And there is no sign of performance degradation or overfitting. [25].

GoogLeNet is the champion of the 2014 ILSVRC Challenge. In order to propose a deeper network, GoogLeNet implements 22 layers and introduces the inception structure. The inception structure increases the width and depth of the network without increasing the computational load. In order to optimize network quality, GoogLeNet adopts Hebbian principle and multi-scale processing [29].

InceptionV3 network is proposed by Szegedy et al, which uses improved Inception Module structure. The improved Inception Module has three structures:  $8 \times 8$ ,  $17 \times 17$  and  $35 \times 35$ . This structure also uses branches in branches. InceptionV3 introduces the idea of Factorization into small convolutions, which turns a larger two-dimensional convolution into two smaller one-dimensional convolutions. This approach can better handle features and reduce the computational load at the same time [26].

Xception network is proposed by Chollet, and it is an improved version of InceptionV3. The main innovation is the introduction of depthwise separable convolutions, which separates channel convolution from spatial convolution. This improves the efficiency of the network. The amount of parameters is equivalent to InceptionV3, but the result is better than InceptionV3 under a large amount of data training [27].

InceptionResNetV1 is proposed by Szegedy et al, which combines the Inception block and the ResNet connection to take advantage of both. While the training speed is fast, the calculation efficiency is also improved. This method has almost the same computational load as InceptionV3, but the convergence speed is faster. [32].

MobileNetV2 is proposed by Sandler et al. The innovation of this method is the introduction of inverted residual with linear bottleneck. The inverse residual first increases the number of channels, then convolves, and then decreases the number of channels. This can reduce memory consumption. And the introduction of linear bottleneck enables better retention of features [30].

A lightweight network called ShuffleNetV2 is proposed by Ma et al, and it uses channel split at the beginning of the block. One part performs three convolution operations, and the other part is directly combined with the results of the previous part, then feature fusion is performed through channel shuffle. This method increases the speed while ensuring accuracy [31].

ViT model is proposed by Dosovitskiy et al, which applies the Transformer applied in the field of natural language processing to the field of computer vision. ViT proves that CNN is not the only option for image classification tasks. Under the training of a large amount of data, the effect of ViT is better than CNN [21].

BoTNet is proposed by Srinivas, which combines self-attention with ResNet. While obtaining local information, it also has the ability to obtain global information. This method replaces the convolutional layer of the three bottleneck blocks behind ResNet with self-attention layers. This reduces the amount of parameters, but the effect is better than ResNet [33].

DeiT is proposed by Touvron et al. The innovation of DeiT is the introduction of distillation token. The distillation token is similar to the ViT class token. It is a token added after the image block sequence. The output after the Transformer

encoder and the output of the teacher model calculate the loss together. The training of DeiT requires less data and less computing resources [34].

T2T-ViT is proposed by Yuan et al. This work proposes a new T2T mechanism based on ViT. T2T mechanism overcomes the shortcomings of the original simple token. It uses a progressive method to structure the image into tokens and model local structural information. T2T-ViT requires fewer parameters than ViT, but achieves better results [35].

### 3. Materials and methods

#### 3.1. Dataset

##### 3.1.1. Dataset description

The public database SIPaKMeD is used to compare the performance of deep learning models. The database contains 4049 separated cervical cell images, all of which are cropped from clustered cell images obtained by CCD camera. These images include five categories, dyskeratotic, koiocytotic, metaplastic, parabasal and superficial-intermediate, where some examples are shown in Fig. 3 [22].

##### 3.1.2. Data setting

The SIPaKMeD database contains 4049 cervical cell images. 60% of the data are randomly selected for training, 20% for validation and the remaining data for testing. Then deep learning models are used to perform 5-class classification experiments on the data. The training set, validation set and test set are shown in Table 1.

##### 3.1.3. Data preprocessing

The size of cervical cell images in the SIPaKMeD database is inconsistent, but the input required by the deep learning models is consistent. In order to discover whether the image scale has an impact on the performance of the models, the cervical cell images (raw data) in the database are standardized and centralized. The standard operation is to check whether the length of the raw data is longer than the width, if so, rotate the raw data by 90 degrees counterclockwise, otherwise no processing is done. The centralization operation is to find the longest side length in all images, and then use zero to supplement all images to square matrices of that length. The standardized and centralized images are called the "standard data", some examples are shown in Fig. 4.

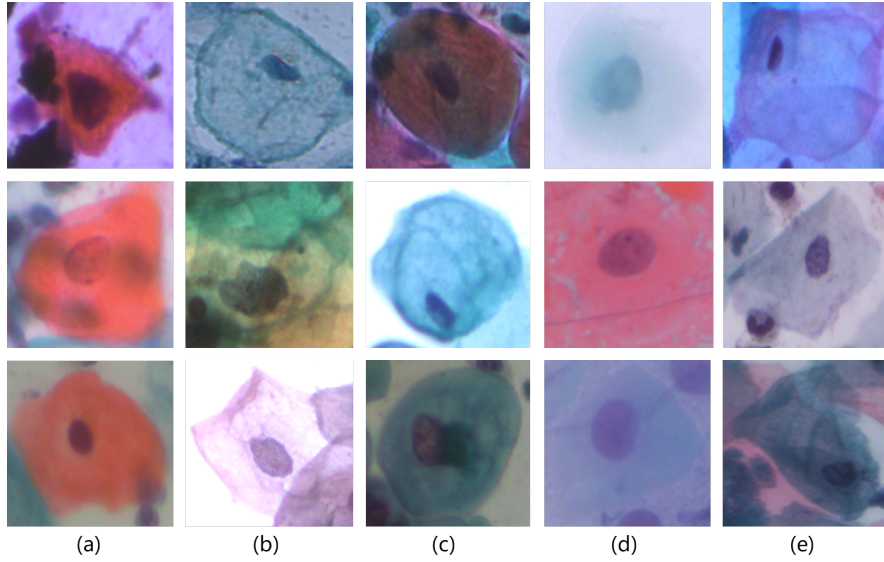


Figure 3: SIPaKMeD database example: (a) Dyskeratotic, (b) Koilocytotic, (c) Metaplastic, (d) Parabasal, (e) Superficial-Intermediate.

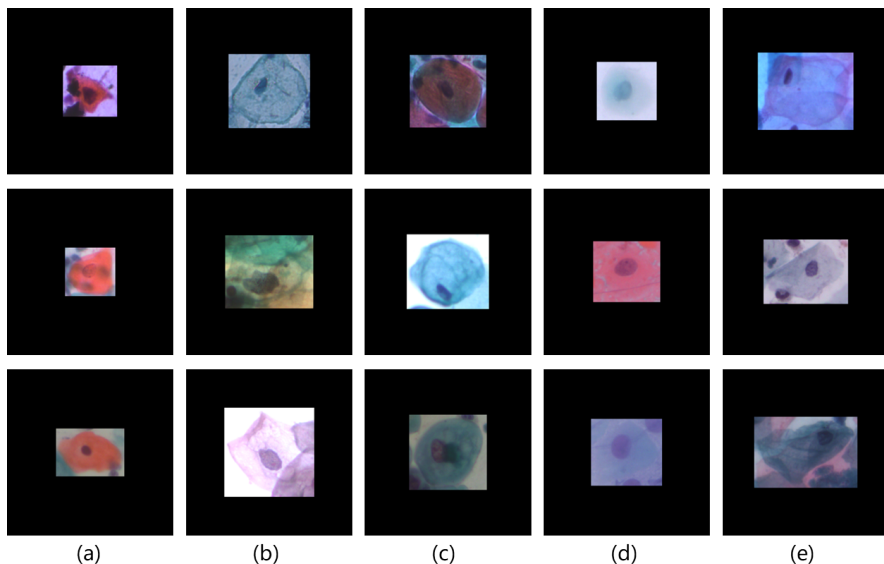


Figure 4: SIPaKMeD standard data example: (a) Dyskeratotic, (b) Koilocytotic, (c) Metaplastic, (d) Parabasal, (e) Superficial-Intermediate.

Table 1: SIPaKMeD data arrangement.

Dataset/Class	Dyskeratotic	Koilocytotic	Metaplastic	Parabasal	Superficial-Intermediate	Total
Training	488	495	476	473	499	2431
Validation	163	165	159	157	166	810
Test	162	165	158	157	166	808
Total	813	822	793	787	831	4049

### 3.2. State of deep learning models

22 deep learning models are used in this robustness comparison experiment. 18 of the models are CNNs, including VGG11 [23], VGG13 [23], VGG16 [23], VGG19 [23], ResNet18 [24], ResNet34 [24], ResNet50 [24], ResNet101 [24], DenseNet121 [25], DenseNet169 [25], InceptionV3 [26], Xception [27], AlexNet [28], GoogLeNet [29], MobileNetV2 [30], ShuffleNetV2x1.0 [31], ShuffleNetV2x0.5 [31], InceptionResNetV1 [32]. Four of the models are VTs, including ViT [21], BoTNet [33], DeiT [34], T2T-ViT [35]. As shown in Table 2, these models are briefly summarized with reference, parameters, the top-1 accuracy on the ImageNet dataset and the major remarks.

### 3.3. Classification using deep learning models

22 deep learning models introduced above are used to perform 5-class classification tasks on cervical cell images in the SIPaKMeD dataset. First, the training set and validation set generated by raw data and standard data are used to train models. Then the test set is used to evaluate the performance of models. The results of the two classifications are compared and analyzed through the obtained evaluation indicators to find out whether the image scale has an impact on the performance of models.

## 4. Experiments and analysis

### 4.1. Experimental setup

This comparative experiment is carried out on a local computer. The running memory of this computer is 32 G. It uses the Win10 Professional operating system and is equipped with an 8 G NVIDIA GeForce RTX 2080 GPU. Python 3.7, Pytorch 1.8.0 and Torchvision 0.9.0 are configured on this computer. In addition, the code runs in the integrated development environment Pycharm Community Edition.

### 4.2. Evaluation method

It is very important to choose an appropriate evaluation method in the comparative experiment. Precision, recall, F1-Score, and accuracy are the most commonly used and most standard evaluation methods in classification experiments [44, 45]. Take the two classification as an example, the prediction is a positive example and it is actually a positive

example, which is called True Positives (TP). The prediction is a positive example but it is actually a negative example called False Positives (FP). The prediction is negative, but it is actually a positive example called False Negatives (FN). The prediction is negative and it is actually a negative example called True Negatives (TN). Precision is the proportion of TP among all predictions that are positive. Recall is the ratio of predicted positive examples to the total number of actual positive examples. F1-Score combines precision and recall. Accuracy is the ratio of the number of correct predictions to the total number of examples. The formulas of the four evaluation methods are shown in Table 3.

### 4.3. Experimental results and analysis

The average precision, average recall, average F1-Score and accuracy are used to evaluate models trained by raw data and standard data. The results are shown in Table 4.

In Table 4, among CNNs trained on raw data, models with very high accuracy are Xception and DenseNet169, which are 97.16% and 96.91% respectively. The model with the lowest accuracy is VGG19, which is 89.50%. The accuracy of the remaining CNNs is also above 90%. In VTs trained on raw data, the model with the highest accuracy is DeiT, which is 96.54%. And the model with the lowest accuracy is BoTNet, which is 87.16%. The accuracy of ViT and T2T-ViT is also around 95%. Among all models trained on raw data, Xception has the highest average precision and average recall of 97.30% and 97.20%. BoTNet has the lowest average precision and average recall of 87.80% and 87.20%.

In CNNs trained on standard data, Xception has the highest accuracy rate of 96.79%. Its average precision and average recall are the highest among all models, with percentages of 97.00% and 96.80%. VGG19 is still the model with the lowest accuracy of 91.35%. In VTs trained on standard data, DeiT has the highest accuracy of 95.30%. T2T-ViT is the model with the lowest accuracy of 90.61%. In addition, its average precision and average recall are the lowest among all models, being 90.70% and 90.70% respectively.

The accuracy of models trained on standard data is the baseline, and the comparison of the accuracy of models trained on raw data and standard data can be seen on the left side of Table 6. In this table, the accuracy of 12 raw data training models is higher than that of standard data training

Table 2: A brief introduction to the deep learning models used in the robustness comparison experiment. (In [%].)

Model	Ref.	Parameters	Top-1 accuracy	Major remarks
VGG11	[23]	133M	69.02	a.The network has deeper layers and uses smaller filters.
VGG13		133M	69.93	
VGG16		138M	71.59	b.Training takes a long time.
VGG19		144M	72.38	
ResNet18	[24]	11.7M	69.76	a.The residual block is introduced.
ResNet34		21.8M	73.31	b.The problem of rapid decline in accuracy due to the increase in the number of network layers is solved.
ResNet50		25.6M	76.13	
ResNet101		44.7M	77.37	
DenseNet121	[25]	8M	74.43	a.A direct connection between any two layers with the same feature map size is introduced.
DenseNet169		14.3M	75.60	b.It can scale to hundreds of layers.
InceptionV3	[26]	23.8M	77.29	a.It uses improved Inception Module. b.It introduces the idea of Factorization into small convolutions.
Xception	[27]	22.9M	79.00	a.It is an improved version of InceptionV3. b.It uses depthwise separable convolutions.
AlexNet	[28]	60M	56.52	a.ReLu activation function is introduced. b.Data augmentation and dropout layers are used to prevent overfitting.
GoogLeNet	[29]	6.8M	69.78	a.It introduces the inception structure. b.It adopts multi-scale processing and Hebbian principle.
MobileNetV2	[30]	3.4M	71.89	a.Inverted residual with linear bottleneck is introduced.
ShuffleNetV2x1.0	[31]	2.3M	69.36	a.It uses channel split at the beginning of the block.
ShuffleNetV2x0.5		1.4M	60.55	
InceptionResNetV1	[32]	8M	78.70	a.It combines the Inception block and the ResNet connection.
ViT	[21]	86M	73.38	a.It applies the Transformer to the field of computer vision. b.It is better than CNN under the training of a large amount of data.
BoTNet	[33]	20.8M	77.00	a.It combines self-attention with ResNet.
DeiT	[34]	5M	72.20	a.Distillation token is introduced. b.The training of DeiT requires less data and computing resources.
T2T-ViT	[35]	4.2M	71.70	a.A new T2T mechanism based on ViT is used.

Table 3: Evaluation metrics

Assessment	Formula
Precision ( $P$ )	$\frac{TP}{TP+FP}$
Recall ( $R$ )	$\frac{TP}{TP+FN}$
F1-Score	$2 \times \frac{P \times R}{P+R}$
Accuracy	$\frac{TP+TN}{TP+TN+FP+FN}$

models. The accuracy of one model is equal and the accuracy of nine models is reduced. Among them, the model with the most increase in accuracy is T2T-ViT, with 3.95%, and the increase rate is 4.36%. BoTNet's accuracy is reduced the most, with 4.69%, and the ratio is 5.11%. The overall trend is that the accuracy of some models increases and some decreases, and the proportion of increase or decrease is not very large.

Then the closed test set in raw data and standard data is used to evaluate the generalization ability of models, as shown in Table 5. In CNNs using the raw data test set, GoogLeNet surpasses Xception, reaching the highest test accuracy of 96.03%, and its average precision and average recall are 96.30% and 96.00%. The test accuracy of VGG19 is still the lowest among CNNs, with the accuracy rate of 88.11%. In VTs using the raw data test set, DeiT's test accuracy is still the highest at 95.42%. BoTNet has the lowest accuracy rate of 84.77%, and its average precision and average recall are the lowest among all models, 85.80% and 84.80% respectively.

In CNNs, using the standard data test set, the highest test accuracy of Xception reaches 96.79%, and its average precision and average recall are 97.00% and 96.80%, respectively. The test accuracy of VGG19 is the lowest among CNNs, with the accuracy of 91.35%. In VTs using the standard data test set, DeiT still has the highest test accuracy at 95.30%. The lowest accuracy rate of T2T-ViT is 90.61%, and its average precision and average recall are the lowest among all models, 90.70% and 90.70% respectively.

The right side of Table 6 compares models accuracy of the test set using raw data and standard data. The accuracy of the test on the standard data is still the baseline. In this table, the accuracy of 12 models tested with raw data is higher than the

results of the standard data test set. The test accuracy of 10 models is reduced. Among them, T2T-ViT increases the most, with an increase of 3.34% and a ratio of 3.78%. BoTNet reduces the most, with a decrease of 6.81%, and a ratio of 7.44%. The overall fluctuation is not very large.

#### 4.4. Extended experiment

##### 4.4.1. Extended experiment on SIPaKMeD dataset: classification with data augmentation

The training set and validation set of the SIPaKMeD dataset mentioned above are augmented, and the data are augmented to four times by rotating 180 degrees, flipping left and right, and flipping up and down. Then the augmented data are standardized and centralized to get standard data. The augmented raw data and standard data are used to train models. The arrangement of data is shown in Table 7.

The classification performance of models on the validation set of SIPaKMeD augmented data is shown in Table 8. In this table, among CNNs trained on raw data, Xception has the highest accuracy, which is 98.45%. Among VTs trained on raw data, DeiT has the highest accuracy of 97.74%. Among CNNs trained on standard data, GoogLeNet surpasses Xception to become the model with the highest accuracy of 97.80%. Among VTs trained on standard data, DeiT still has the highest accuracy rate.

The classification performance of models on the test set of SIPaKMeD augmented data is shown in Table 9. In this table, In CNNs trained on raw data, ResNet18 has the highest accuracy, which is 97.15%. In VTs trained on raw data, ViT has the highest accuracy rate of 95.54%. In CNNs trained on standard data, GoogLeNet is the model with the highest accuracy, 97.40%. In VTs trained on standard data, DeiT also has the highest accuracy rate.

The comparison of the training results between the augmented raw data and standard data in the SIPaKMeD dataset is shown in Table 10. On the left side of this table are comparison results on the validation set. The accuracy of 16 raw data training models is higher than that of standard data training models. The accuracy of six models is reduced. Among them, the model with the greatest increase in accuracy is T2T-ViT, which has the increase of 2.32% and the ratio of 2.46%. The accuracy of VGG19 reduces the most, down 1.79%, with the

Table 4: The classification performance of models on the **validation** set of SIPaKMeD data. (In [%].)

Models	Raw data				Standard data			
	Avg. P	Avg. R	Avg. F1	Accuracy	Avg. P	Avg. R	Avg. F1	Accuracy
VGG11	94.50	94.50	94.50	94.44	95.30	95.10	95.20	95.06
VGG13	94.00	93.80	93.90	93.82	94.40	94.00	94.10	93.95
VGG16	90.70	90.10	90.20	90.12	93.30	93.40	93.30	93.33
VGG19	89.70	89.50	89.60	89.50	91.60	91.30	91.40	91.35
ResNet18	96.70	96.70	96.70	96.66	95.30	95.30	95.30	95.30
ResNet34	95.60	95.40	95.50	95.43	95.40	95.20	95.20	95.18
ResNet50	94.70	94.50	94.50	94.56	95.10	95.00	95.00	94.93
ResNet101	94.60	94.60	94.60	94.56	94.20	94.30	94.20	94.19
DenseNet121	95.40	95.30	95.30	95.30	95.70	95.70	95.70	95.67
DenseNet169	97.00	96.90	96.90	96.91	95.60	95.60	95.60	95.55
InceptionV3	94.10	94.00	94.00	93.95	95.40	95.50	95.40	95.43
Xception	97.30	97.20	97.20	97.16	97.00	96.80	96.80	96.79
AlexNet	95.10	95.10	95.10	95.06	94.30	94.30	94.20	94.19
GoogLeNet	96.10	96.10	96.10	96.04	96.20	96.10	96.00	96.04
MobileNetV2	95.40	95.40	95.40	95.40	94.70	94.70	94.70	94.69
ShuffleNetV2x1.0	95.50	95.30	95.30	95.30	93.70	93.70	93.70	93.70
ShuffleNetV2x0.5	93.20	93.00	93.00	92.96	91.90	91.80	91.70	91.72
InceptionResNetV1	95.80	95.70	95.70	95.67	96.00	96.00	95.90	95.92
ViT	95.40	95.40	95.30	95.30	93.30	93.20	93.20	93.20
BoTNet	87.80	87.20	87.30	87.16	91.90	91.90	91.90	91.85
DeiT	96.70	96.60	96.60	96.54	95.50	95.40	95.40	95.30
T2T-ViT	94.60	94.60	94.60	94.56	90.70	90.70	90.60	90.61

Table 5: The classification performance of models on the **test set** of SIPaKMeD data. (In [%].)

Models	Raw data				Standard data			
	Avg. P	Avg. R	Avg. F1	Accuracy	Avg. P	Avg. R	Avg. F1	Accuracy
VGG11	93.70	93.60	93.60	93.56	93.30	92.80	92.90	92.82
VGG13	91.60	91.20	91.30	91.21	93.50	93.20	93.30	93.19
VGG16	89.80	89.20	89.30	89.23	92.80	92.90	92.80	92.82
VGG19	88.60	88.10	88.30	88.11	91.00	90.90	90.90	90.84
ResNet18	95.60	95.50	95.60	95.54	93.80	93.80	93.80	93.81
ResNet34	94.30	94.00	94.10	94.05	94.10	94.00	94.00	93.93
ResNet50	93.10	92.80	92.80	92.82	94.90	94.70	94.70	94.67
ResNet101	92.30	92.00	92.00	91.95	93.70	93.70	93.60	93.68
DenseNet121	95.80	95.70	95.70	95.66	95.20	94.90	95.00	94.92
DenseNet169	95.80	95.70	95.70	95.66	95.30	95.20	95.20	95.17
InceptionV3	93.20	93.00	93.10	92.94	94.00	93.70	93.70	93.68
Xception	96.10	95.90	95.90	95.91	95.20	94.50	94.60	94.55
AlexNet	92.00	91.90	91.90	91.83	93.50	93.50	93.40	93.44
GoogLeNet	96.30	96.00	96.10	96.03	94.30	94.10	94.10	94.05
MobileNetV2	93.80	93.70	93.70	93.68	93.10	93.20	93.20	93.19
ShuffleNetV2x1.0	92.30	91.90	91.90	91.83	92.80	92.80	92.70	92.69
ShuffleNetV2x0.5	92.70	92.30	92.40	92.32	90.40	90.40	90.40	90.34
InceptionResNetV1	93.80	93.70	93.70	93.68	94.70	94.60	94.60	94.55
ViT	93.60	93.60	93.60	93.56	92.10	91.90	91.90	91.83
BoTNet	85.80	84.80	84.90	84.77	91.50	91.60	91.50	91.58
DeiT	95.50	95.40	95.50	95.42	94.20	94.30	94.20	94.18
T2T-ViT	91.90	91.70	91.70	91.70	88.30	88.40	88.30	88.36

Table 6: Comparison table of raw data training results and standard data training results in SIPaKMeD dataset. (Standard data training result is the baseline and the metric for comparison is accuracy). (In [%].)

Models	Validation			Test		
	Up/down	Change	Ratio	Up/down	Change	Ratio
VGG11	down	-0.62	-0.65	up	+0.74	+0.80
VGG13	down	-0.13	-0.14	down	-1.98	-2.13
VGG16	down	-3.21	-3.44	down	-3.59	-3.87
VGG19	down	-1.85	-2.03	down	-2.73	-3.01
ResNet18	up	+1.36	+1.43	up	+1.73	+1.84
ResNet34	up	+0.25	+0.26	up	+0.12	+0.13
ResNet50	down	-0.37	-0.39	down	-1.85	-1.95
ResNet101	up	+0.37	+0.39	down	-1.73	-1.85
DenseNet121	down	-0.37	-0.39	up	+0.74	+0.78
DenseNet169	up	+1.36	+1.42	up	+0.49	+0.52
InceptionV3	down	-1.48	-1.55	down	-0.74	-0.79
Xception	up	+0.37	+0.38	up	+1.36	+1.44
AlexNet	up	+0.87	+0.92	down	-1.61	-1.72
GoogLeNet	equal	0.00	0.00	up	+1.98	+2.11
MobileNetV2	up	+0.74	+0.78	up	+0.49	+0.53
ShuffleNetV2x1.0	up	+1.60	+1.71	down	-0.86	-0.93
ShuffleNetV2x0.5	up	+1.24	+1.35	up	+1.98	+2.19
InceptionResNetV1	down	-0.25	-0.26	down	-0.87	-0.92
ViT	up	+2.10	+2.25	up	+1.73	+1.88
BoTNet	down	-4.69	-5.11	down	-6.81	-7.44
DeiT	up	+1.24	+1.30	up	+1.24	+1.31
T2T-ViT	up	+3.95	+4.36	up	+3.34	+3.78

Table 7: SIPaKMeD augmented data arrangement.

Dataset/Class	Dyskeratotic	Koilocytotic	Metaplastic	Parabasal	Superficial-Intermediate	Total
Training	1952	1980	1904	1892	1996	9724
Validation	652	660	636	628	664	3240
Test	162	165	158	157	166	808
Total	2766	2805	2698	2677	2826	13772

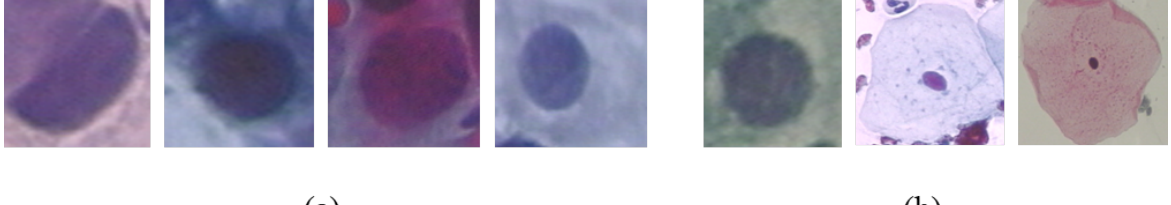


Figure 5: Herlev dataset example: (a) Abnormal, (b) Normal. (From left to right: Carcinoma *in situ*, Normal squamous, Intermediate squamous, Columnar, Mild dysplasia, Moderate dysplasia, Severe dysplasia.)

ratio of 1.89%. On the right side of this table are the comparison results of the models on the test set. The accuracy of eight raw data training models is higher than that of standard data training models. The accuracy of 13 models is reduced, and one model is equal. The model with the largest improvement is ViT, which has the increase of 2.60% and the ratio of 2.80%. The accuracy of VGG19 reduces the most, down 2.60%, with the ratio of 2.73%. The overall trend is still that the accuracy of some models increases, and some decreases. In either case, all of the floating ratio are greatly reduced.

#### 4.4.2. Extended experiment on Herlev dataset

The Herlev dataset contains 917 cell images, including seven categories: Normal squamous, Intermediate squamous, Columnar, Mild dysplasia, Moderate dysplasia, Severe dysplasia and Carcinoma *in situ*. Furthermore, these seven categories can also be divided into normal and abnormal types, where the normal type contains 242 images, and the abnormal type contains 675 images, some examples are shown in Fig. 5 [46].

Herlev dataset is used for two-class classification tasks. 60% of the data are randomly selected for training, 20% of the data for validation, and 20% of the data for testing. Because the amount of data is relatively small, the data are augmented to four times by rotating 180 degrees, flipping left and right and flipping up and down. The augmented data

arrangement is shown in Table 11. Then the augmented data are standardized and centralized to get standard data. The augmented raw data and standard data are used as the input of models for classification.

The two-class classification performance of models on the validation set of Herlev augmented data is shown in Table 12. In this table, among CNNs trained on raw data, ResNet18 has the highest accuracy, which is 93.03%. Among VTs trained on raw data, DeiT has the highest accuracy of 93.16%. Among CNNs trained on standard data, Xception is the model with the highest accuracy of 94.80%. Among VTs trained on standard data, T2T-ViT has the highest accuracy rate of 87.84%.

The two-class classification performance of models on the test set of Herlev augmented data is shown in Table 13. In this table, In CNNs trained on raw data, GoogLeNet has the highest accuracy, which is 93.44%. In VTs trained on raw data, DeiT has the highest accuracy rate of 93.44%. In CNNs trained on standard data, DenseNet121 is the model with the highest accuracy, 95.08%. In VTs trained on standard data, T2T-ViT has the highest accuracy rate of 90.16%.

The comparison of the training results between the augmented raw data and standard data in the Herlev dataset is shown in Table 14. On the left side of this table are comparison results on the validation set. The accuracy of 15 raw data training models is higher than that of standard data train-

Table 8: The classification performance of models on the **validation set** of SIPaKMeD augmented data. (In [%].)

Models	Raw data				Standard data			
	Avg. P	Avg. R	Avg. F1	Accuracy	Avg. P	Avg. R	Avg. F1	Accuracy
VGG11	96.70	96.50	96.60	96.57	96.90	96.70	96.80	96.72
VGG13	96.90	96.90	96.90	96.88	96.80	96.70	96.70	96.69
VGG16	95.40	95.40	95.40	95.37	96.30	96.30	96.20	96.26
VGG19	93.30	93.10	93.10	93.05	95.00	94.90	94.90	94.84
ResNet18	98.20	98.20	98.20	98.14	97.30	97.20	97.20	97.22
ResNet34	97.50	97.50	97.50	97.50	96.90	96.90	96.90	96.91
ResNet50	97.30	97.30	97.30	97.28	97.50	97.40	97.40	97.37
ResNet101	97.10	97.10	97.10	97.09	97.10	97.10	97.10	97.06
DenseNet121	97.50	97.50	97.50	97.46	97.30	97.30	97.20	97.25
DenseNet169	96.30	96.20	96.20	97.56	97.30	97.30	97.30	97.31
InceptionV3	96.80	96.80	96.70	96.72	97.10	97.00	97.00	97.00
Xception	98.50	98.50	98.40	98.45	97.50	97.30	97.40	97.34
AlexNet	96.50	96.40	96.40	96.41	96.10	96.10	96.10	96.04
GoogLeNet	97.50	97.40	97.50	97.43	97.80	97.80	97.80	97.80
MobileNetV2	97.30	97.30	97.30	97.31	97.00	97.00	96.90	96.94
ShuffleNetV2x1.0	97.70	97.60	97.70	97.65	96.40	96.30	96.30	96.32
ShuffleNetV2x0.5	96.50	96.50	96.50	96.45	95.50	95.30	95.30	95.30
InceptionResNetV1	97.70	97.70	97.70	97.68	97.60	97.70	97.60	97.62
ViT	96.60	96.40	96.50	96.41	94.30	94.20	94.20	94.13
BoTNet	89.30	89.20	89.20	89.13	89.30	89.10	89.10	89.07
DeiT	97.80	97.80	97.70	97.74	96.30	96.10	96.10	96.08
T2T-ViT	96.80	96.80	96.80	96.82	94.70	94.50	94.50	94.50

Table 9: The classification performance of models on the **test set** of SIPaKMeD augmented data. (In [%].)

Models	Raw data				Standard data			
	Avg. P	Avg. R	Avg. F1	Accuracy	Avg. P	Avg. R	Avg. F1	Accuracy
VGG11	96.20	96.20	96.10	96.03	95.20	94.80	94.90	94.80
VGG13	94.70	94.60	94.60	94.55	96.30	96.30	96.30	96.28
VGG16	94.10	93.90	94.00	93.93	95.30	95.10	95.20	95.17
VGG19	93.10	92.50	92.70	92.57	95.30	95.20	95.20	95.17
ResNet18	97.20	97.20	97.20	97.15	96.90	96.80	96.80	96.78
ResNet34	96.30	96.20	96.20	96.16	96.10	96.00	96.10	96.03
ResNet50	95.60	95.60	95.60	95.54	96.20	96.20	96.10	96.03
ResNet101	96.00	95.90	95.90	95.91	95.80	95.70	95.70	95.66
DenseNet121	96.90	96.90	96.90	96.90	97.10	97.10	97.00	97.02
DenseNet169	96.30	96.20	92.00	96.16	96.60	96.50	96.50	96.53
InceptionV3	95.40	95.20	95.20	95.17	96.80	96.80	96.80	96.78
Xception	97.00	97.10	97.00	97.02	96.10	96.10	95.80	95.79
AlexNet	95.10	94.90	94.90	94.92	95.60	95.70	95.70	95.66
GoogLeNet	96.80	96.80	96.80	96.78	97.50	97.40	97.40	97.40
MobileNetV2	96.50	96.60	96.50	96.53	96.80	96.80	96.80	96.78
ShuffleNetV2x1.0	96.90	96.80	96.80	96.78	96.10	96.10	96.10	96.03
ShuffleNetV2x0.5	95.30	95.20	95.20	95.17	95.90	95.80	95.80	95.79
InceptionResNetV1	95.10	95.10	95.00	95.04	97.20	97.20	97.20	97.15
ViT	95.80	95.60	95.60	95.54	93.10	93.00	93.00	92.94
BoTNet	87.60	87.60	87.50	87.62	88.90	89.00	88.90	88.98
DeiT	95.10	95.00	95.00	94.92	95.00	94.90	95.00	94.92
T2T-ViT	94.50	94.50	94.40	94.43	92.20	92.10	92.10	92.07

Table 10: Comparison table of training results between the augmented raw data and standard data in SIPaKMeD dataset. (The augmented standard data training result is the baseline and the metric for comparison is accuracy). (In [%].)

Models	Validation			Test		
	Up/down	Change	Ratio	Up/down	Change	Ratio
VGG11	down	-0.15	-0.16	up	+1.23	+1.30
VGG13	up	+0.19	+0.20	down	-1.73	-1.80
VGG16	down	-0.89	-0.93	down	-1.24	-1.30
VGG19	down	-1.79	-1.89	down	-2.60	-2.73
ResNet18	up	+0.92	+0.95	up	+0.37	+0.38
ResNet34	up	+0.59	+0.61	up	+0.13	+0.14
ResNet50	down	-0.09	-0.09	down	-0.49	-0.51
ResNet101	up	+0.03	+0.03	up	+0.25	+0.26
DenseNet121	up	+0.21	+0.22	down	-0.12	-0.12
DenseNet169	up	+0.25	+0.26	down	-0.37	-0.38
InceptionV3	down	-0.28	-0.29	down	-1.61	-1.66
Xception	up	+1.11	+1.14	up	+1.23	+1.28
AlexNet	up	+0.37	+0.39	down	-0.74	-0.77
GoogLeNet	down	-0.37	-0.38	down	-0.62	-0.64
MobileNetV2	up	+0.37	+0.38	down	-0.25	-0.26
ShuffleNetV2x1.0	up	+1.33	+1.38	up	+0.75	+0.78
ShuffleNetV2x0.5	up	+1.15	+1.21	down	-0.62	-0.65
InceptionResNetV1	up	+0.06	+0.06	down	-2.11	-2.17
ViT	up	+2.28	+2.42	up	+2.60	+2.80
BoTNet	up	+0.06	+0.07	down	-1.36	-1.53
DeiT	up	+1.66	+1.73	equal	0.00	0.00
T2T-ViT	up	+2.32	+2.46	up	+2.36	+2.56

Table 11: Herlev augmented data arrangement.

Dataset/Class	Normal	Abnormal	Total
Training	584	1620	2204
Validation	192	540	732
Test	48	135	183
Total	824	2295	3119

ing models. The accuracy of seven models is reduced. Among them, DeiT has the largest increase in accuracy, with the increase of 2.32% and the ratio of 2.46%. The accuracy of VGG19 reduces the most, down 15.02%, with the ratio of 16.92%. On the right side of this table are the comparison results of the models on the test set. The accuracy of 14 raw data training models is higher than that of standard data training models, and the accuracy of eight models is reduced. The model with the largest improvement is ViT, which has the increase of 7.10% and the ratio of 8.33%. The accuracy of VGG19 reduces the most, down 14.75%, with the ratio of 16.66%. Except for the VGG19 model, the accuracy of other models does not fluctuate too much.

## 5. Discussion

In this study, 22 deep learning models are used to classify multi-scale images, and comparison results are obtained based on evaluation indicators, as shown in Table 6.

In Table 6, the VGG series network does not perform well in processing directly resized raw data. According to the structure, the smaller filter may be the cause of the poor effect. In addition, the performance of the VGG network gradually decreases as the number of layers increases, and the performance of the network with a small number of layers is better. In the ResNet series network that uses the residual block, the one with fewer network layers has more advantages and better performance for processing raw data. In the DenseNet series network, the direct connection is introduced between any two layers with the same feature map size, and the performance of models is not affected by the number of layers. This should also be the reason for the better performance on raw data. GoogLeNet introduces the inception structure and adopts the Hebbian principle and multi-scale processing, which performs better on raw data processing. The reason for InceptionV3’s poor performance on raw data

should be that one large two-dimensional convolution is replaced with two small one-dimensional convolutions. As an improved version of InceptionV3, Xception introduces depthwise separable convolution, which improves performance while also performing better on raw data. AlexNet, which introduces the ReLu activation function, performs worse on raw data processing. Lightweight networks such as MobileNet and ShuffleNet have more advantages in processing raw data.

In VTs, except for BoTNet, the other models have a better effect on raw data. It can be because Transformer pays more attention to global information and lacks local perception. BoTNet is a combination of ResNet and Transformer, which obtains global and local information, and has a good effect on processing standard data. Among these 22 models, some models are better at processing raw data, and some are better at processing standard data. So it shows that deep learning method is very robust to multi-scale images.

Furthermore, the augmented SIPaKMeD dataset are used as the input of models for classification to test the impact of the size of the training set on the training of deep learning models. The comparison results are shown in Table 10. After the augmented data training, the DenseNet series network and lightweight network processing raw data are less effective than processing standard data. The rest is basically the same. Therefore, after augmenting the training data, some redundant information appears, resulting a negative impact on some models.

Additionally, the augmented Herlev dataset are used as the input of models for classification. The comparison results are shown in Table 14. The number of augmented Herlev dataset is almost the same as the number of SIPaKMeD unaugmented dataset, so the conclusion is almost consistent with the above. This further shows that deep learning method is robust to the changes of image sizes.

According to the experimental and extended experimental results, in the CNN and VT models, some models have good effects on raw data, and some have good effects on standard data, showing that deep learning method is very robust to the size changes of images.

## 6. Conclusion and future work

The image input required by the deep learning model is usually consistent, but the size of many

Table 12: The two-class classification performance of models on the **validation set** of Herlev augmented data. (In [%].)

Models	Raw data				Standard data			
	Avg. P	Avg. R	Avg. F1	Accuracy	Avg. P	Avg. R	Avg. F1	Accuracy
VGG11	89.50	85.40	87.20	90.57	86.70	87.50	87.00	89.89
VGG13	88.20	79.40	82.40	87.84	89.40	84.00	86.20	90.02
VGG16	85.20	81.90	83.40	87.70	84.50	82.70	83.50	87.56
VGG19	36.90	50.00	42.40	73.77	89.00	81.20	84.00	88.79
ResNet18	93.20	88.60	90.60	93.03	90.70	86.90	88.60	91.53
ResNet34	94.00	85.60	88.80	92.07	88.90	88.40	88.60	91.25
ResNet50	89.10	88.90	89.00	91.53	93.20	90.30	91.60	93.71
ResNet101	88.70	86.40	87.40	90.57	89.50	88.00	88.60	91.39
DenseNet121	90.50	87.50	88.80	91.66	90.50	89.90	90.20	92.48
DenseNet169	91.90	89.50	90.60	92.89	90.10	88.70	89.40	91.93
InceptionV3	89.40	88.60	89.00	91.53	90.40	83.80	86.40	90.30
Xception	91.60	88.90	90.20	92.62	94.70	91.70	93.00	94.80
AlexNet	88.00	79.50	82.50	87.84	88.90	82.80	85.20	89.34
GoogLeNet	89.80	89.10	89.40	91.93	90.70	84.60	87.10	90.71
MobileNetV2	90.10	87.50	88.70	91.53	90.50	81.80	84.90	89.48
ShuffleNetV2x1.0	89.70	86.10	87.60	90.84	91.70	83.20	86.30	90.43
ShuffleNetV2x0.5	89.10	85.90	87.30	90.57	89.00	75.60	79.30	86.47
InceptionResNetV1	91.50	87.60	89.20	92.07	90.10	88.40	89.20	91.80
ViT	86.80	88.90	87.80	90.30	87.70	72.20	75.80	84.69
BoTNet	86.40	79.70	82.20	87.43	84.70	70.40	73.60	83.30
DeiT	90.60	92.40	91.40	93.16	88.40	76.90	80.40	86.88
T2T-ViT	85.60	83.80	84.60	88.38	88.20	79.40	82.40	87.84

Table 13: The two-class classification performance of models on the **test set** of Herlev augmented data. (In [%].)

Models	Raw data				Standard data			
	Avg. P	Avg. R	Avg. F1	Accuracy	Avg. P	Avg. R	Avg. F1	Accuracy
VGG11	86.00	81.80	83.60	87.97	85.50	80.80	82.70	87.43
VGG13	89.90	81.20	84.30	89.07	90.70	87.70	89.00	91.80
VGG16	86.10	80.10	82.40	87.43	86.60	84.50	85.50	89.07
VGG19	36.90	50.00	42.40	73.77	90.50	79.40	83.00	88.52
ResNet18	93.20	86.80	89.40	92.34	91.50	89.80	90.60	92.89
ResNet34	92.40	84.70	87.60	91.25	88.10	86.00	86.90	90.16
ResNet50	89.10	88.00	88.60	91.25	93.20	86.80	89.40	92.34
ResNet101	91.00	88.70	89.80	92.34	88.70	91.10	89.80	91.80
DenseNet121	91.70	88.10	89.70	92.34	96.00	91.30	93.40	95.08
DenseNet169	91.50	89.80	90.60	92.89	89.60	89.10	89.30	91.80
InceptionV3	87.50	84.90	86.10	89.61	89.70	85.60	87.40	90.71
Xception	92.80	88.50	90.40	92.89	89.10	88.00	88.60	91.25
AlexNet	91.60	85.30	87.80	91.25	86.50	82.80	84.40	88.52
GoogLeNet	91.10	92.20	91.60	93.44	90.70	83.30	86.10	90.16
MobileNetV2	90.40	85.00	87.10	90.71	89.00	81.90	84.60	89.07
ShuffleNetV2x1.0	92.40	84.70	87.60	91.25	90.70	83.30	86.10	90.16
ShuffleNetV2x0.5	90.60	89.40	90.00	92.34	90.50	79.40	83.00	88.52
InceptionResNetV1	90.80	86.00	88.00	91.25	88.60	87.00	87.80	90.71
ViT	89.70	90.80	90.20	92.34	86.80	73.90	77.40	85.24
BoTNet	91.30	81.60	84.90	89.61	90.10	78.40	82.00	87.97
DeiT	91.50	91.50	91.60	93.44	88.50	78.00	81.40	87.43
T2T-ViT	84.70	83.80	84.20	87.90	91.70	82.60	85.90	90.16

Table 14: Comparison table of training results between the augmented raw data and standard data in Herlev dataset. (The augmented standard data training result is the baseline and the metric for comparison is accuracy). (In [%].)

Models	Validation			Test		
	Up/down	Change	Ratio	Up/down	Change	Ratio
VGG11	up	+0.68	+0.76	up	+0.54	+0.62
VGG13	down	-2.18	-2.42	down	-2.73	-2.97
VGG16	up	+0.14	+0.16	down	-1.64	-1.84
VGG19	down	-15.02	-16.92	down	-14.75	-16.66
ResNet18	up	+1.50	+1.64	down	-0.55	-0.59
ResNet34	up	+0.82	+0.90	up	+1.09	+1.21
ResNet50	down	-2.18	-2.33	down	-1.09	-1.18
ResNet101	down	-0.82	-0.90	up	+0.54	+0.59
DenseNet121	down	-0.82	-0.89	down	-2.74	-2.88
DenseNet169	up	+0.96	+1.04	up	+1.09	+1.19
InceptionV3	up	+1.23	+1.36	down	-1.10	-1.21
Xception	down	-2.18	-2.30	up	+1.64	+1.80
AlexNet	down	-1.50	-1.68	up	+2.73	+3.08
GoogLeNet	up	+1.22	+1.34	up	+3.28	+3.64
MobileNetV2	up	+2.05	+2.29	up	+1.64	+1.84
ShuffleNetV2x1.0	up	+0.41	+0.45	up	+1.09	+1.21
ShuffleNetV2x0.5	up	+4.10	+4.74	up	+3.82	+4.32
InceptionResNetV1	up	+0.27	+0.29	up	+0.54	+0.60
ViT	up	+5.61	+6.62	up	+7.10	+8.33
BoTNet	up	+4.13	+4.96	up	+1.64	+1.86
DeiT	up	+6.28	+7.23	up	+6.01	+6.87
T2T-ViT	up	+0.54	+0.61	down	-2.26	-2.51

clinical medical images is inconsistent. The internal information is lost after resizing the image directly, so it is unreasonable. However, many studies directly resize images, and the results are still robust. In order to find a reasonable explanation, cervical cells are used as an example to test the robustness of deep learning method. After processing the data, raw data and standard data are obtained to compare 22 deep learning models. The final conclusion is that deep learning method is still robust to multi-scale images.

Recently, the popular Transformer surpasses the CNN network in the field of computer vision. In this study, Transformer does not show amazing results, and BoTNet combined with Transformer and ResNet does not perform well on cervical cell images, either. We assume that combining Xception, which performs well in this study, with Transformer may result in better performance. Transformer focus on global information, so we can fuse Transformer and classical local features to obtain better classification performance. In the future, we can also try to use more new VTs to classify medical images, and make improvements and supplements based on the structure of the model. In addition, standardization and centralization can be used as data preprocessing, which may increase the accuracy of the model.

## References

- [1] G. Bugdayci, M. B. Pehlivan, M. Basol, O. M. Yis, Roles of the systemic inflammatory response biomarkers in the diagnosis of cancer patients with solid tumors, *Experimental Biomedical Research* 2 (1) (2019) 37–43.
- [2] J. Ferlay, M. Ervik, F. Lam, M. Colombet, L. Mery, M. Piñeros, A. Znaor, I. Soerjomataram, F. Bray, Global cancer observatory: cancer today, Lyon, France: International Agency for Research on Cancer.
- [3] Chaturvedi, K. Anil, Epidemiology and clinical aspects of hpv in head and neck cancers, *Head Neck Pathol* 6 (1 Supplement) (2012) 16–24.
- [4] H. U. Bernard, R. D. Burk, Z. Chen, K. V. Doorslaer, H. Z. Hausen, E. Villiers, Classification of papillomaviruses (pvs) based on 189 pv types and proposal of taxonomic amendments., *Virology* 401 (1) (2010) 70–79.
- [5] E. J. Crosbie, M. H. Einstein, S. Franceschi, H. C. Kitchener, Human papillomavirus and cervical cancer, *The Lancet* 382 (9895) (2013) 889–899.
- [6] W. F. Cheng, Human papillomavirus vaccine for cervical cancer: Where are we now?, *Taiwanese Journal of Obstetrics Gynecology* 44 (3) (2005) 391–391.
- [7] S. S. De, M. Diaz, X. Castellsague, G. Clifford, L. Bruni, Worldwide prevalence and genotype distribution of cervical human papillomavirus dna in women with normal cytology: a meta-analysis., *Lancet Infectious Diseases* 7 (7) (2007) 453–459.
- [8] F. X. Bosch, A. N. Burchell, M. Schiffman, A. R. Giuliano, S. de Sanjose, L. Bruni, G. Tortolero-Luna, S. K. Kjaer, N. Muñoz, Epidemiology and natural history of human papillomavirus infections and type-specific implications in cervical neoplasia, *Vaccine* 26 (2008) K1–K16.
- [9] T. Šarenac, M. Mikov, Cervical cancer, different treatments and importance of bile acids as therapeutic agents in this disease, *Frontiers in pharmacology* 10 (2019) 484.
- [10] D. Saslow, D. Solomon, H. W. Lawson, M. Killackey, S. L. Kulasingam, J. Cain, F. A. Garcia, A. T. Moriarty, A. G. Waxman, D. C. Wilbur, et al., American cancer society, american society for colposcopy and cervical pathology, and american society for clinical pathology screening guidelines for the prevention and early detection of cervical cancer, *CA: a cancer journal for clinicians* 62 (3) (2012) 147–172.
- [11] E. Davey, A. Barratt, L. Irwig, S. F. Chan, A. M. Saville, Effect of study design and quality on unsatisfactory rates, cytology classifications, and accuracy in liquid-based versus conventional cervical cytology: a systematic review., *Lancet* 367 (9505) (2006) 122–132.
- [12] A. Gençtav, S. Aksoy, S. Önder, Unsupervised segmentation and classification of cervical cell images, *Pattern Recognition* 45 (12) (2012) 4151–4168.
- [13] M. M. Rahaman, C. Li, X. Wu, Y. Yao, S. Qi, A survey for cervical cytopathology image analysis using deep learning, *IEEE Access* PP (99) (2020) 1–1.
- [14] E. Bengtsson, P. Malm, Screening for cervical cancer using automated analysis of pap-smears, *Computational and Mathematical Methods in Medicine*, 2014,(2014-3-20) 2014 (2014) 842037.
- [15] Y. LeCun, Y. Bengio, G. Hinton, Deep learning, *nature* 521 (7553) (2015) 436–444.
- [16] F. Xing, L. Yang, Robust nucleus/cell detection and segmentation in digital pathology and microscopy images: A comprehensive review, *IEEE Rev Biomed Eng* (2016) 234–263.
- [17] I. Goodfellow, Y. Bengio, A. Courville, Y. Bengio, *Deep learning*, Vol. 1, MIT press Cambridge, 2016.
- [18] M. S. Landau, L. Pantanowitz, Artificial intelligence in cytopathology: a review of the literature and overview of commercial landscape, *Journal of the American Society of Cytopathology* 8 (4) (2019) 230–241.
- [19] G. Hinton, Deep learning—a technology with the potential to transform health care, *Jama* 320 (11) (2018) 1101–1102.
- [20] Y. Lecun, K. Kavukcuoglu, C. Farabet, Convolutional networks and applications in vision, in: *Proceedings of 2010 IEEE International Symposium on Circuits and Systems*, 2010.
- [21] A. Dosovitskiy, L. Beyer, A. Kolesnikov, D. Weissenborn, X. Zhai, T. Unterthiner, M. Dehghani, M. Minderer, G. Heigold, S. Gelly, et al., An image is worth 16x16 words: Transformers for image recognition at scale, *arXiv preprint arXiv:2010.11929*.
- [22] M. E. Plissiti, P. Dimitrakopoulos, G. Sfikas, C. Nikou, O. Krikoni, A. Charchanti, Sipakmed: A new dataset for feature and image based classification of normal and pathological cervical cells in pap smear images, in: *2018 25th IEEE International Conference on Image Processing (ICIP)*, IEEE, 2018, pp. 3144–3148.

[23] K. Simonyan, A. Zisserman, Very deep convolutional networks for large-scale image recognition, arXiv preprint arXiv:1409.1556.

[24] K. He, X. Zhang, S. Ren, J. Sun, Deep residual learning for image recognition, in: Proceedings of the IEEE conference on computer vision and pattern recognition, 2016, pp. 770–778.

[25] G. Huang, Z. Liu, L. Van Der Maaten, K. Q. Weinberger, Densely connected convolutional networks, in: Proceedings of the IEEE conference on computer vision and pattern recognition, 2017, pp. 4700–4708.

[26] C. Szegedy, V. Vanhoucke, S. Ioffe, J. Shlens, Z. Wojna, Rethinking the inception architecture for computer vision, IEEE (2016) 2818–2826.

[27] F. Chollet, Xception: Deep learning with depthwise separable convolutions, in: 2017 IEEE Conference on Computer Vision and Pattern Recognition (CVPR), 2017.

[28] O. Russakovsky, J. Deng, H. Su, J. Krause, S. Satheesh, S. Ma, Z. Huang, A. Karpathy, A. Khosla, M. Bernstein, et al., Imagenet large scale visual recognition challenge, *International journal of computer vision* 115 (3) (2015) 211–252.

[29] C. Szegedy, W. Liu, Y. Jia, P. Sermanet, S. Reed, D. Anguelov, D. Erhan, V. Vanhoucke, A. Rabinovich, [ieee 2015 ieee conference on computer vision and pattern recognition (cvpr) - boston, ma, usa (2015.6.7-2015.6.12)] 2015 ieee conference on computer vision and pattern recognition (cvpr) - going deeper with convolutions (2015) 1–9.

[30] M. Sandler, A. Howard, M. Zhu, A. Zhmoginov, L.-C. Chen, Mobilenetv2: Inverted residuals and linear bottlenecks, in: Proceedings of the IEEE conference on computer vision and pattern recognition, 2018, pp. 4510–4520.

[31] N. Ma, X. Zhang, H.-T. Zheng, J. Sun, Shufflenet v2: Practical guidelines for efficient cnn architecture design, in: Proceedings of the European conference on computer vision (ECCV), 2018, pp. 116–131.

[32] C. Szegedy, S. Ioffe, V. Vanhoucke, A. Alemi, Inception-v4, inception-resnet and the impact of residual connections on learning, in: Proceedings of the AAAI Conference on Artificial Intelligence, Vol. 31, 2017.

[33] A. Srinivas, T.-Y. Lin, N. Parmar, J. Shlens, P. Abbeel, A. Vaswani, Bottleneck transformers for visual recognition, arXiv preprint arXiv:2101.11605.

[34] H. Touvron, M. Cord, M. Douze, F. Massa, A. Sablayrolles, H. Jégou, Training data-efficient image transformers & distillation through attention, arXiv preprint arXiv:2012.12877.

[35] L. Yuan, Y. Chen, T. Wang, W. Yu, Y. Shi, F. E. Tay, J. Feng, S. Yan, Tokens-to-token vit: Training vision transformers from scratch on imagenet, arXiv preprint arXiv:2101.11986.

[36] J. Hyeon, H.-J. Choi, K. N. Lee, B. D. Lee, Automating papanicolaou test using deep convolutional activation feature, in: 2017 18th IEEE International Conference on Mobile Data Management (MDM), IEEE, 2017, pp. 382–385.

[37] B. Taha, J. Dias, N. Werghi, Classification of cervical-cancer using pap-smear images: a convolutional neural network approach, in: Annual Conference on Medical Image Understanding and Analysis, Springer, 2017, pp. 261–272.

[38] H. Wieslander, G. Forslid, E. Bengtsson, C. Wahlby, J.-M. Hirsch, C. Runow Stark, S. Kecheril Sadanandan, Deep convolutional neural networks for detecting cellular changes due to malignancy, in: Proceedings of the IEEE International Conference on Computer Vision Workshops, 2017, pp. 82–89.

[39] S. Gautam, N. Jith, A. K. Sao, A. Bhavsar, A. Nataraajan, et al., Considerations for a pap smear image analysis system with cnn features, arXiv preprint arXiv:1806.09025.

[40] Y. Promworn, S. Pattanasak, C. Pintavirooj, W. Piyawattanametha, Comparisons of pap smear classification with deep learning models, in: 2019 IEEE 14th International Conference on Nano/Micro Engineered and Molecular Systems (NEMS), IEEE, 2019, pp. 282–285.

[41] L. D. Nguyen, R. Gao, D. Lin, Z. Lin, Biomedical image classification based on a feature concatenation and ensemble of deep cnns, *Journal of Ambient Intelligence and Humanized Computing* (2019) 1–13.

[42] Kurnianingsih, K. Allehaibi, L. E. Nugroho, Widyan, T. Mantoro, Segmentation and classification of cervical cells using deep learning, *IEEE Access PP* (99) (2019) 1–1.

[43] L. Zhang, L. Lu, I. Nogues, R. M. Summers, S. Liu, J. Yao, Deeppap: deep convolutional networks for cervical cell classification, *IEEE journal of biomedical and health informatics* 21 (6) (2017) 1633–1643.

[44] Y. Xie, F. Xing, X. Kong, H. Su, L. Yang, Beyond classification: structured regression for robust cell detection using convolutional neural network, in: International conference on medical image computing and computer-assisted intervention, Springer, 2015, pp. 358–365.

[45] P. Sukumar, R. Gnanamurthy, Computer aided detection of cervical cancer using pap smear images based on adaptive neuro fuzzy inference system classifier, *Journal of Medical Imaging and Health Informatics* 6 (2) (2016) 312–319.

[46] J. Jantzen, J. Norup, G. Dounias, B. Bjerregaard, Pap-smear benchmark data for pattern classification, *Nature inspired Smart Information Systems (NiSIS 2005)* (2005) 1–9.